Regular Article

ANALYTICAL
AND BIOANALYTICAL
CHEMISTRY
RESEARCH

Published by the
Iranian Chemical Society

***Anal. Bioanal. Chem. Res.**, Vol. 11, No. 2, 177-189, April 2024.*

Investigation of Isotherm, Thermodynamic, and Kinetics of Bovine Serum Albumin Adsorption onto MCM-41@LDH

Forough Karami[a,b], Ardeshir Shokrollahi[a,*] and Salimeh Abbasi[a]

[a]*Department of Chemistry, Yasouj University, Yasouj 75918-74831, Iran*

[b]*Central Research Laboratory, School of Medicine, Shiraz University of Medical Sciences, Shiraz, Iran*

(Received 21 November 2023, Accepted 21 January 2024)

The survey of protein adsorption is important due to the significant application of proteins in food, medicine, biotechnology, environment, and separation science. Therefore, in the current investigation, the adsorption of bovine serum albumin (BSA) onto a functionalized mesoporous (MCM-41) using layered double hydroxide (MCM-41@LDH) was investigated under different conditions such as the amount of adsorbent, pH of the solution, contact time, and protein concentration. The optimization process was carried out using central composite design (CCD). After the characterization of the modified mesoporous, more investigations were conducted to assess the adsorption of BSA onto MCM-41@LDH, including adsorption isotherm, kinetics, and thermodynamics. It was revealed that Freundlich isotherm and second-order kinetics provided the best fit for support of MCM-41@LDH. The values of Gibbs free energy (ΔG°), enthalpy (ΔH°), and entropy (ΔS°) were determined as -3100.47 kJ mol^{-1} K^{-1} (at 298.15 K), -3101.12 kJ mol^{-1}, and -0.002 kJ mol^{-1}, respectively. According to CCD analysis and desirability function of 1.0, the optimal conditions for BSA adsorption were determined to be a pH value of 4.50, BSA concentration of 250 mg l^{-1}, support amount of 0.016 g, and contact time of 55 min. The obtained findings can be used for purification, separation, and removal of BSA from complex samples.

Keywords: Bovine serum albumin, Central composite design, Freundlich, Layered double hydroxide, MCM-41

INTRODUCTION

Albumin as the chief soluble protein of mammalian plasma is recognized for its significant properties in the transportation and delivery of numerous compounds, such as drugs, hormones, amino acids, and fatty acids [1]. Bovine serum albumin (BSA) containing 583 amino acids [2] is applied for vaccine formulation, immunological experiments [3], as a drug, as an antigen [4], and as a standard molecule [5,6].

The study of interactions between proteins and sorbent surfaces has drawn considerable attention in various sciences and applications such as biomedical engineering, biotechnology, improvement of biomineralization methods, and control of drug delivery systems, which can be useful in the fields of biosensors, bioassay, bioseparation, biocatalysis, and food processing [7-15]. To do these, it is noteworthy that the kinetics and thermodynamics of the mentioned interactions should be surveyed. Kinetics studies allow us to obtain information about the adsorption rate, the performance of the sorbent, and the mechanisms of mass transfer [16]. The survey of kinetics and thermodynamics provides necessary information about the mechanism of protein adsorption and its arrangement on an adsorbent surface [15].

Protein chromatography has shown great attention due to the significant role of proteins in the industries of food and pharmaceutical. In the separation of proteins, both the appropriate type of the stationary phase and the mobile phase affect the chromatography separation [17]. In this regard, nanoparticles as an adsorbent are suitable because of their

*Corresponding author. E-mail: ashokrollahi@yu.ac.ir

homogeneous particle size and high surface area. The interaction between the adsorbent surface and proteins is of great interest in various fields such as nanotechnology, biochemistry, biotechnology, environment, and biomedicine [18]. Therefore, the physical and chemical structures of the adsorbent affect protein adsorption.

Layered double hydroxides (LDHs) or anionic clays are the subject of intense research because numerous components and metal-anionic compounds can be used for the synthesis of LDH [19], which causes great applications in sewage treatment [19], ion exchange [19], polymers stabilization, pharmaceuticals, food industries, and catalytic activities.

Different porous materials have been reported, which can be classified into three categories based on their pore diameters [20]: microporous materials with dimensions of less than 2 nm [21], mesoporous silica with dimensions of 2-50 nm [22], and macroporous materials with pore diameters higher than 50 nm [23]. Among these compounds, mesoporous solids are more efficient because of their high surface area [24], tunable dimensions [25], and high porosities [26]. Mesoporous solids can be categorized as SBA [27], MCM [28], FSM [29], TUD [30], and HMS [31]. Among these types of mesoporous, MCM-41 mesoporous silica has been subjected to extensive studies due to its ordered porous structure, high surface area, large pore volume, thick walls, and good stability, making it suitable for applications in catalysis, drug delivery, protein immobilization, adsorption, and separation [32]. The adsorption capacity of MCM-41 is moderately low. Therefore, to provide high removal and increased adsorption capacity, more potent and novel supports need to be synthesized.

Although there have been several publications discussing the adsorption of BSA on various materials, there is no experimental data regarding the adsorption of BSA onto MCM-41@LDH. In previous studies, nanosized magnetic particles (Fe_3O_4) [33], single-walled carbon nanotubes [34], and graphene nanoplatelets [35] were utilized to investigate the adsorption of BSA as the model protein [34].

The objective of our current investigation is to study BSA adsorption, which is a complex process and involves various interactions, such as hydrophobic, hydrophilic, and hydrogen bonding. To achieve this, modification of MCM-41 was done using LDH (MCM-41@LDH) based on our previous report [36]. To account for many environmental parameters that affect the adsorption process, the chief factors in the experiment were conducted at numerous BSA concentrations, contact time, pH, and amount of adsorbent. Furthermore, the isotherm, kinetics, and thermodynamics of adsorption were investigated to identify the adsorption capacity of the adsorbent and recognize the adsorption mechanism of BSA onto MCM-41@LDH, which can be appropriate for protein delivery, biosensor, chromatographic, and separation applications.

EXPERIMENTAL

Materials

All materials were of analytical grade. Trisodium phosphate dodecahydrate ($Na_3PO_4.12H_2O$), magnesium nitrate hexahydrate ($Mg(NO_3)_2.6H_2O$), aluminum nitrate nonahydrate ($Al(NO_3)_3.9H_2O$), ammonia (NH_3), cetyl trimethyl ammonium bromide (CTAB), tetraethyl orthosilicate (TEOS), and ammonium hydroxide (NH_4OH) were purchased from Merck Company (Darmstadt, Germany). BSA powder was obtained from Sigma-Aldrich Company (St. Louis, MO, USA). Deionized water with an electrical resistance of 18.2 MΩ.cm was obtained using a Milli-Q system.

Instruments

To record the absorbance of samples, Agilent Technologies Cary Series 100 UV/VIS Spectrophotometer was used. The spectra of samples were recorded using Fourier transform infrared spectroscopy (FTIR-460, JASCO, Japan) between the ranges of 4000-400 cm^{-1} using a KBr disc.

Synthesis and Modification of Nanomaterial

Step 1: Synthesize of MCM-41

Preparation of MCM-41@LDH was carried out according to the previous reports [36-38]. To synthesize MCM-41, we dissolved 4.000 g of CTAB in 1000 ml of 1.1 M ammonium hydroxide to get a clear solution. Next, we added 16 ml of TEOS, a source of silicon, drop by drop with gentle stirring for 24 h at room temperature. After that, we filtered the product, washed it with water, and let it dry at

room temperature for 48 h, resulting in the formation of MCM-41. To remove the CTAB from the structure of MCM-41, we then performed a calcination procedure at 823 K for 24 h [37,38]. Finally, we modified the obtained product using LDH.

Step 2: Synthesis of MCM-41@LDH

Briefly, after the synthesis of MCM-41 (step 1), a defined amount of MCM-41 was suspended in deionized water and stirred. Subsequently, the addition of $Mg(NO_3)_2.6H_2O$ and $Al(NO_3)_3.9\ H_2O$ to MCM-41 solution was done, adjusting pH was performed using ammonia solution, and then stirred. After filtering and washing using deionized water, drying the filter paper was done at a temperature of 100 °C to get MCM-41@LDH.

Adsorption Experiment onto MCM-41@LDH

A stock solution of BSA (1 mg ml^{-1}) was prepared in sodium phosphate buffer (20 mM). Subsequently, different solutions of BSA ranging from 100-700 mg l^{-1} were prepared. In the following, the absorbance of standard solutions was studied using a spectrophotometer. The adsorption of BSA was investigated using a central composite design (CCD) in which different concentrations of BSA, amounts of adsorbent, contact time, and pH ranges were surveyed using central composite design (CCD) via the software package Design-Expert version 7.0.0 trial. The details of the desired parameters can be found in Tables 1 and 2. Generally, for each level from Table 2, a specific amount of MCM-41@LDH was mixed with a known protein concentration (10 ml) at a particular pH and contact time. After that, the centrifugation was done at 4000 rpm for 20 min and the supernatant was studied at a λ_{max} of 280 nm *via* UV/Vis spectrophotometer (Fig. 1). Similar analyses were performed for MCM-41@SiO_2-NH-pydc [38] and functionalized GO using Schiff base [39]. However, due to the low percentage of adsorption (data were not shown), other experiments such as isotherm, kinetics, and thermodynamics were not investigated. Finally, the adsorption percentage of BSA onto MCM-41@LDH (A%) was obtained according to the following Eq. (1):

$$\%A = \frac{(A_0 - A_e) \times 100}{A_0} \quad (1)$$

where A_0 and A_e are described as the initial and final absorbance of BSA at the λ_{max} of protein (280 nm).

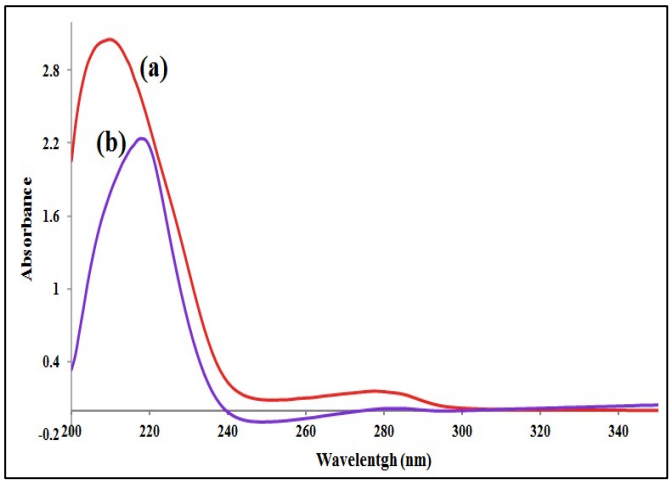

Fig. 1. UV-VIS spectra of (a) BSA before and (b) after adsorption onto MCM-41@LDH (Conditions: BSA concentration of 250 mg l^{-1}, pH 4.50, support amount of 0.016 g, and contact time of 55 min).

Table 1. Designed Parameters for the Response Surface Quadratic Model

Factor	Low value	Central value	High value
pH	4.5	6.0	7.5
Concentration of BSA (mg l^{-1})	250	400	550
Amount of MCM-41@LDH (g)	0.015	0.03	0.035
Contact time (min)	55	95	135

Table 2 Experimental Conditions from Central Composite Design for the Adsorption of BSA

Run	pH	Concentration of BSA (mg l^{-1})	Amount of MCM-41@LDH (g)	Contact time (min)
1	4.50	550.00	0.035	135.00
2	4.50	250.00	0.035	135.00
3	7.50	250.00	0.015	135.00
4	7.50	550.00	0.015	55.00
5	7.50	550.00	0.015	135.00
6	6.00	400.00	0.025	175.00
7	6.00	100.00	0.025	95.00
8	7.50	550.00	0.035	55.00
9	4.50	250.00	0.015	135.00
10	4.50	250.00	0.035	55.00
11	7.50	550.00	0.035	135.00
12	9.00	400.00	0.025	95.00
13	4.50	550.00	0.015	55.00
14	6.00	400.00	0.025	95.00
15	7.50	250.00	0.035	135.00
16	4.50	550.00	0.035	55.00
17	4.50	550.00	0.015	135.00
18	6.00	400.00	0.025	95.00
19	6.00	400.00	0.025	95.00
20	6.00	700.00	0.025	95.00
21	6.00	400.00	0.025	95.00
22	6.00	400.00	0.005	95.00
23	6.00	400.00	0.045	95.00
24	6.00	400.00	0.025	95.00
25	4.50	250.00	0.015	55.00
26	7.50	250.00	0.015	55.00
27	6.00	400.00	0.025	15.00
28	3.00	400.00	0.025	95.00
29	6.00	400.00	0.025	95.00
30	7.50	250.00	0.035	55.00

Isotherm, Kinetics, and Thermodynamic of BSA Adsorption onto MCM-41@LDH

Regarding the spectroscopic data (%A, adsorption percentage), the study of isotherm, kinetics, and thermodynamics of BSA was performed onto MCM-41@LDH due to the good adsorption percentage of BSA. The survey of isotherm was performed at room temperature following the adsorption experiments (section 2.4). Various concentrations of BSA (150, 250, 350, and 500 mg l^{-1}) were used at a pH of 4.50, support amount of 0.016 g, and contact time of 55 min. All parameters, except for concentration, were chosen based on optimized points. For the kinetics

experiment at the optimized conditions, samples were collected at 2-minute intervals up to 16 min. In the following, samples were collected at 15-minute intervals up to 55 min. After centrifugation, the amount of adsorbed BSA onto MCM-41@LDH was measured using the UV/Vis spectrophotometer technique.

In order to survey the thermodynamics of protein onto MCM-41@LDH, the experiment was accomplished according to the optimum conditions at several temperatures comprising 15, 25, 35, and 45 °C.

Analysis of Data

Response surface methodology (RSM), developed by Box and Wilson, has been used to identify the key factors that affect the experiments. This methodology is an effective tool for experimental design [40]. In the current investigation, Design-Expert software version 7.0.0 trial for Windows was applied to design and survey relationships among criteria factors. In order to data analysis, statistical analysis of variance (ANOVA) was used. Also, three-dimensional response surfaces were plotted to evaluate how the response varies with the desired parameters (Fig. 2).

RESULTS AND DISCUSSION

Characterization of MCM-41@LDH before and after Adsorption of BSA

To identify the structure of MCM-41@LDH, FTIR analysis was performed. Other techniques including scanning electron microscopy (SEM), X-ray diffraction (XRD), and energy-dispersive X-ray spectrometry (EDX) for characterization of MCM-41@LDH were reported in our previous research [36].

FTIR spectrum of MCM-41@LDH before and after adsorption of BSA is displayed in Fig. 3. The absorption peaks around 1034 and 582 cm^{-1} are attributed to the MCM-41 structure. The sharp peak at 1034 cm^{-1} corresponds to the Si-O stretching band and is considered the fingerprint region of MCM-41 [41]. Additionally, the wide absorption peak at 3408 cm^{-1} presents the stretching vibration of Si-OH and the existence of H_2O in the interlayer of the LDH structure [42]. The peak around 1377 cm^{-1} is referred to NO_3^- group within the structure of LDH, which was reduced after BSA adsorption [43]. The main absorption band of BSA appears at 1622 cm^{-1} which is assigned to the amide group. Also, the peak of 1622 cm^{-1} overlaps with the bending vibration of H_2O in the LDH structure [43]. After loading of BSA, the desired peaks of BSA decreased indicating that the protein adsorption onto MCM-41@LDH was effective.

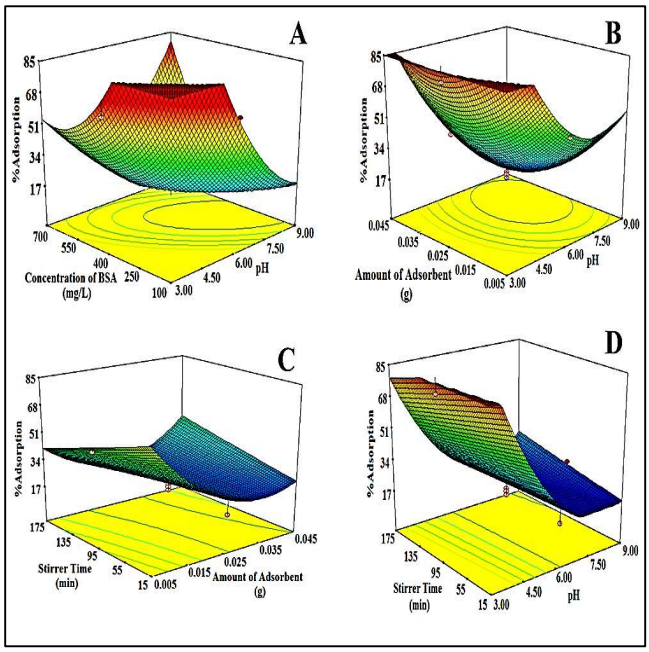

Fig. 2. Three-dimensional response surfaces for BSA adsorption.

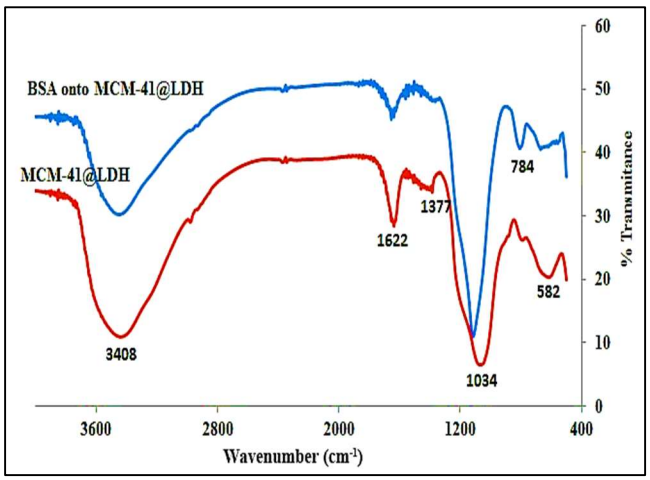

Fig. 3. FTIR spectrum of BSA before and after adsorption onto MCM-41@LDH.

Central Composite Design

As presented in Table 1, a CCD was employed to investigate four effective variables in the adsorption process: pH, concentration of BSA, amount of MCM-41@LDH, and contact time. A total of 30 experiments were conducted based on the designed program (Tables 1 and 2). The characteristics and responses of each run are shown in Table 2. Analysis of variance (ANOVA) in Table 3 indicates the significance of the designed model and the main interactions between parameters. The F-value (Table 3) for the Model (23.7) is significant. Model terms with p-values less than 0.0500 are considered significant: A, B, C, AB, BC, A^2, B^2, and C^2. The value of F-value for Lack of Fit (1.85) suggests its insignificance compared to pure error. The high value of adequated precision (14.398), which represents the signal-to-noise ratio, indicates an adequate and desirable signal. Finally, a quadratic equation was obtained using the values of the coefficients, which are as follows:

$$\text{Response} = 471.80449 - 76.33898\,A - 0.60989\,B - 2004.51823\,C - 0.47782\,D + 0.050347\,AB - 18.70833\,AC + 0.036260\,AD - 3.92542\,BC + 1.38021E\text{-}004\,BD + 6.85469\,CD + 3.54458\,A^2 + 4.33403E\text{-}004\,B^2 + 51190.62500\,C^2 + 4.16016E\text{-}005\,D^2 \quad (2)$$

where the response is the adsorption percent of BSA and A, B, C, and D are presented as the pH of the mixture, the concentration of BSA, the amount of adsorbent, and contact time, respectively.

Table 3. Analysis of Variance Results for Response Surface Quadratic Model

Source	Sum of squares	D.F[a]	Mean square	F-Value	p-value Prob > F	
Model	14939.78	14	1067.13	23.70	< 0.0001	Significant
A (pH)	6168.66	1	6168.66	136.99	< 0.0001	
B (Concentration of BSA)	1148.03	1	1148.03	25.49	0.0001	
C (Amount of MCM-41@LDH)	544.26	1	544.26	12.09	0.0034	
D (Contact time)	25.52	1	25.52	0.57	0.4632	
AB	2053.22	1	2053.22	45.60	< 0.0001	
AC	1.26	1	1.26	0.028	0.8694	
AD	75.73	1	75.73	1.68	0.2143	
BC	554.72	1	554.72	12.32	0.0032	
BD	10.97	1	10.97	0.24	0.6287	
CD	120.29	1	120.29	2.67	0.1230	
A^2	1744.61	1	1744.61	38.74	< 0.0001	
B^2	2608.26	1	2608.26	57.92	< 0.0001	
C^2	718.76	1	718.76	15.96	0.0012	
D^2	0.12	1	0.12	2.699E-003	0.9593	
Residual	675.46	15	45.03			
Lack of fit	531.62	10	53.16	1.85	0.2582	Not significant
Pure error	143.84	5	28.77			
Total	15615.23	29				

[a]Degree of freedom.

In order to realize the acquired results, three-dimensional response surface graphs are illustrated in Fig. 2. To understand the best experimental conditions, a desirability parameter of 1.0 was selected as the maximum response. As demonstrated in Fig. 2, a decrease in parameters of pH, BSA concentration, and amount of support caused to increasing response. But, it is obvious that contact time is almost constant, which means that its effect is low, probably. Consequently, according to the achieved data and desirability function of 1.0, the following conditions were determined: pH value of 4.50, BSA concentration of 250 mg l^{-1}, support amount of 0.016 g, and contact time of 55 min.

Optimization of Effective Parameters

With regard to the important role of pH on the surface chemistry of proteins (conformational variations) and adsorbent, in the current investigation, this factor was studied over a range of 3.0-9.0 by CCD. The relationship between pH and BSA concentration, the amount of MCM-41@LDH, and contact time were shown in three-dimensional graphs (Fig. 2A, 2B, and 2D). As depicted in Fig. 2 (A, B, and D), the percentage of adsorption decreased with increasing pH and remained constant within the range of 3-4.5. The highest signal was achieved at a pH range of 3-4.50, which is near the BSA isoelectric point (pI = 4.7). At this pH range, the analyte has insignificant structural changes. The pI of a protein is attributed to the pH at which the protein charge is zero. Therefore, proteins show different behavior at various pHs: they are neutral at pH = pI, positively charged at pH < pI, and negatively charged at pH > pI [44]. The pH_{pzc} (Point of Zero Charge) for MCM-41@LDH is 7.8 [45], which means that at this pH, the charge of the adsorbent is positive. This leads to the formation of electrostatic interactions between MCM-41@LDH and the negatively charged carboxylic acid groups of the protein. Conversely, at high pH values, both the adsorbent and protein carry a negative charge. Thus, only hydrogen bonding is responsible for the adsorption of BSA. As a result, the adsorption process is facilitated by the formation of hydrogen bonding and electrostatic interactions between BSA and the adsorbent. Consequently, pH = 4.50 was selected as the optimum pH.

BSA concentration ranging from 100-700 mg l^{-1} was investigated. As seen from Fig. 2A, increasing the concentration was caused by the decreasing signal. The highest adsorption was achieved in the range of 100-400 mg l^{-1}, which might be concluded that at high concentrations of BSA, the saturation has occurred for the definite amount of adsorbent. So, the amount of 250 mg l^{-1} was suggested by the software.

In the following, the adsorption process of MCM-41@LDH was studied using CCD with an amount ranging from 0.005 to 0.05 g. As demonstrated in Fig. 2C, regarding the specified adsorption capacity for each adsorbent, the adsorption signal increases with decreasing amount of MCM-41@LDH. Considering this, an amount of 0.016 g was selected as the best weight. The effect of contact time as another variable was studied ranging from 15 to 175 min. From Fig. 2C & D, it can be observed that the variation of contact time is almost negligible, indicating that this parameter had a low effect, probably. The observed effect is compatible with the insignificant *p*-value of 0.4632 obtained from Table 3 which showed the contact time had no important effect. So, the best time for BSA adsorption was found as 55 min.

BSA Adsorption Isotherm onto MCM-41@LDH

Various isotherm models have been used to explain the adsorption equilibrium of the desired process. In this study, we investigated Langmuir, Freundlich, Temkin, and Dubinin-Radushkevich models to evaluate the adsorption capacity of MCM-41@LDH. The equilibrium equations for BSA adsorption on MCM-41@LDH are shown in Table 4. By considering of high correlation coefficients (R^2) of 0.963 for the Freundlich model, it is concluded that this model showed appropriate fitting to the obtained results. It seems that the BSA adsorption onto MCM-41@LDH is heterogeneous due to the application of this model for heterogeneous procedures. The Freundlich model explains that the ratio of molecule adsorbed to the concentration of molecule is a function of the solution [46]. The empirical equation of Freundlich isotherm is described by Eq. (3) [46]:

$$\ln q_e = \ln K_f + \left(\frac{1}{n}\right) \ln C_e \quad (3)$$

where K_f and n are assumed as Freundlich constants, which are considered as the adsorption capacity and adsorption intensity of a typical process, respectively. The value of K_f

Table 4. Various Isotherm Models for BSA Adsorption onto MCM-41@LDH

Isotherm model	Achieved equation	Parameters	Obtained amount of parameters
Langmuir [46] $\frac{C}{q} = \frac{1}{K\,q_m} + \frac{C}{q_m}$	$y = 0.0009x + 0.144$	q_m	1111.111
		K	0.006
		R^2	0.339
Freundlich [46] $\ln q_e = \ln K_f + \left(\frac{1}{n}\right)\ln C_e$	$y = 1.190x + 0.999$	n	0.840
		K_f	2.71
		R^2	0.963
Temkin [51] $q_e = B_1 \ln K_t + B_1 \ln C_e$	$y = 132.77x - 263.16$	B_1	132.77
		K_t	0.137
		R^2	0.870
Dubinin-Radushkevich [52] $\ln q_e = \ln Q_m - B\varepsilon^2$	$y = -3E-05x + 5.4671$	Q_m	236.77
		E	129.01
		B	-3E-05
		R^2	0.787

C_e: Concentration of BSA at equilibrium time (mg l^{-1}), q_e: BSA adsorbed dosage at equilibrium time (mg g^{-1}), q_m: maximum adsorption capacity (mg g^{-1}), K: Langmuir constant (l mg^{-1}), K_f and n: Freundlich coefficients, K_t: equilibrium binding constant, (M^{-1}), B_1: the constant related to adsorption heat, Q_m: Dubinin-Radushkevich constant (mol g^{-1}), B: the parameter related to average sorption free energy (kJ mol^{-1}), ε: surface potential.

represents the adsorption capacity or affinity of the solid surface for the analyte [47]. Therefore, a large value of K_f points to a high interaction. The slope of line (1/n) is in the range of 0-1 when this value gets near 0, it shows high heterogeneity for the surface of the adsorbent [48]. For 1/n < 1 and 1/n > 1, an ideal Freundlich isotherm and favorable adsorption process are obtained, respectively [49]. In current research, 1/n is above 1 indicating supportive adsorption of BSA onto adsorbent takes place. The Freundlich graph for BSA adsorption on MCM-41@LDH is shown in Fig. 4.

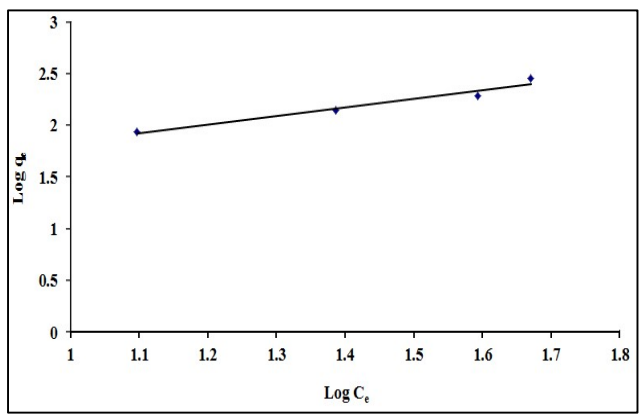

Fig. 4. Freundlich isotherm model for BSA adsorption on MCM-41@LDH (experimental conditions: BSA concentrations of 150, 250, 350, and 500 mg l^{-1} at pH 4.50, amount of support 0.016 g, and contact time of 55 min).

BSA Adsorption Kinetics onto MCM-41@LDH

The first-order, second-order kinetics, intra-particle diffusion, and Elovich models were investigated to explain the mechanism of BSA adsorption. Table 5 displays the kinetics equations and important factors for the adsorption of BSA. It seems that the kinetics model for the adsorption of BSA agrees with the second-order due to the high value of R^2 indicating a linear relationship between t/q_t and time. The second-order model is presented as Eq. (4) [50]:

$$\frac{t}{q_t} = \frac{1}{k_2 q_{eq}^2} + \frac{1}{q_{eq}} t \quad (4)$$

Table 5. Different Kinetics Models for the Adsorption of BSA onto MCM-41@LDH

Kinetics model	Achieved equation	Parameters	Calculated parameters
First-order kinetics [53] $Log(q_{eq} - q_t) = Log\ q_{eq} - (k_1/2.303)t$	$y = -0.1281x + 2.812$	k_1 (g mg^{-1} min^{-1})	0.295
		q_{eq} (mg g^{-1})	648.933
		R^2	0.574
Second-order kinetics [50] $t/q_t = 1/k_2.q_{eq}^2 + t/q_{eq}$	$y = 0.007x + 0.0269$	k_2 (g mg^{-1} min^{-1})	0.001
		q_{eq} (mg g^{-1})	147.05
		R^2	0.992
Intra-particle diffusion [54] $q_{t=K_{dif}t^{0.5}+C}$	$y = 10.972x + 58.311$	K_{dif} (mg g^{-1}min$^{-0.5}$)	10.972
		C	58.311
		R^2	0.971
Elovich [55] $q_t = \frac{1}{\beta}\ln(\alpha\beta) + \frac{1}{\beta}\ln t$	$y = 17.416x + 59.587$	β (g mg^{-1})	0.057
		α (mg g^{-1}min^{-1})	533.139
		R^2	0.872

k_1: rate constant for the first-order kinetics (min^{-1}), q_{eq}: amount of BSA adsorbed at equilibration time (mg g^{-1}), R^2: correlation coefficient, q_t: amount of BSA adsorbed at time t (mg g^{-1}), k_2: rate constant for the second-order kinetics (g mg^{-1} min^{-1}), K_{dif}: intraparticle diffusion rate constant (mg g^{-1} min$^{-0.5}$), C: intercept, α: rate constant for initial adsorption (mg g^{-1} min^{-1}), β: desorption rate constant (g mg^{-1}).

Where k_2, q_{eq}, and q_t are attributed to the rate constant of the second-order kinetics, values of adsorbed BSA onto support at equilibration and t time, respectively. A linear relationship between the plot of $\frac{t}{q_t}$ *versus* time (t) was observed in Fig. 5, in which the rate constant (k_2) and equilibration amount of protein (q_{eq}) were obtained from the slope and intercept of the equation, respectively. The experimental q_{eq} value was found to be 136.97 mg g^{-1}, which is close to the expected theoretical q_{eq} amount from the second-order kinetics (147.05 mg g^{-1}). This result suggests that the proposed model is probably suitable for the adsorption of BSA onto MCM-41@LDH. It was observed that the rate constant of the first order was higher than the similar parameter for the second order, which was in accord with Kopac *et al.* and Amin *et al.* [34,46]. This finding could be related to the adsorption of BSA on the exterior surface of the adsorbent at the primary time of process causing the rate of the adsorption process to be very rapid [34]. In the following, the saturation occurred for the external surface of MCM-41@LDH. Thus, the molecules of protein enter into the pores of the adsorbent followed by adsorption *via* the internal surface, which increases the diffusion resistance and decreases in diffusion rate [34].

BSA Adsorption Thermodynamic onto MCM-41@LDH

Thermodynamic parameters such as Gibbs free energy (ΔG°), enthalpy (ΔH°), and entropy (ΔS°) were calculated to identify the spontaneity of the adsorption process using the following equations:

$$\Delta G^\circ = \Delta H^\circ - T\Delta S^\circ \quad (5)$$

and

$$\Delta G^\circ = -RT \ln K \quad (6)$$

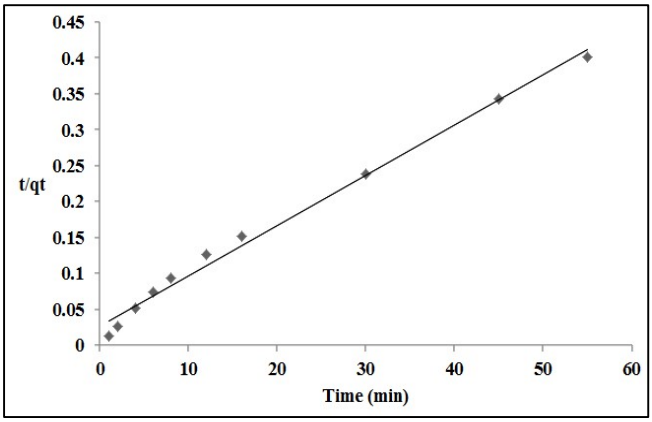

Fig. 5. Second-order kinetics plot for BSA onto MCM-41@LDH in time intervals of 2 min up to 16 min followed by 15 min up to 55 min (Conditions: BSA concentration of 250 mg l^{-1}, pH 4.50, amount of support 0.016 g, and contact time of 55 min).

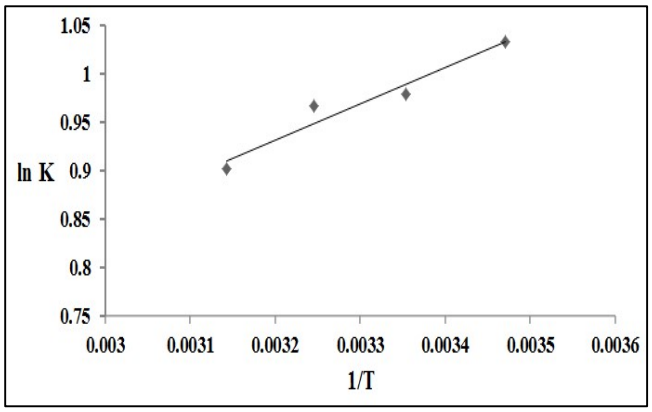

Fig. 6. Thermodynamic curve for adsorption of BSA on MCM-41@LDH at numerous temperatures comprising 15, 25, 35, and 45 °C (Conditions: BSA concentration of 250 mg l^{-1}, pH 4.50, amount of adsorbent 0.016 g, and contact time of 55 min).

where K describes the thermodynamic equilibrium constant, which is the ratio of the equilibrium amount of BSA onto the adsorbent to that in solution and is also, identified by plotting $\ln\frac{q_{eq}}{C_{eq}}$ *versus* q_{eq} (Fig. 6). The slope and intercept of the linear graph for lnK against 1/T can be used to calculate the values of ΔH° and ΔS° for the adsorption process, respectively. Table 6 provides the calculated values of ΔG°, ΔH°, and ΔS° for the adsorption of BSA onto MCM-41@LDH. The amounts of ΔH° and ΔS° were found to be -3101.12 and -0.002 (kJ mol^{-1}), respectively. The negative values of ΔH° and ΔG° indicate the adsorption process is exothermal and spontaneous, respectively. Additionally, the negative value of ΔS° suggests an increase in order degree upon the protein adsorption.

Comparison of BSA Adsorption with other Adsorbents

Similar experiments for the sorbents of MCM-41@SiO_2-NH-pydc [38] and functionalized GO with Schiff base [39] at the optimized conditions of BSA onto MCM-41@LDH were done. Adsorption of BSA onto GO Schiff base had caused 23.6%, because functionalized GO with Schiff base showed slow kinetics. However, more investigations (increasing contact time) did not reveal a good signal. Also, it was established that no significant adsorption was observed for BSA onto MCM-41@SiO_2-NH-pydc, probably due to the adsorption of MCM-41@SiO_2-NH-pydc at the λ_{max} of 280 nm. Moreover, as indicated in Table 7, a comparison of some adsorption parameters with other adsorbents revealed that MCM-41@LDH has the highest q_{eq} (147.05 mg g^{-1}) and also, the lowest time to reach equlibration (55 min). So, among different sorbents, it is concluded that MCM-41@LDH is the best support for BSA.

CONCLUSIONS

It is concluded that both entropic and enthalpic factors affect the adsorption of BSA onto MCM-41@LDH. As an overall result, the protein type, chemistry of the adsorbent surface, conditions of solution, surface topology of adsorbent, and pH of solution are considered effective factors, which influence the thermodynamic and kinetics of protein adsorption.

Various experiments such as UV-visible spectrophotometry and FTIR analyses were conducted to confirm the strong interaction between BSA and MCM-41@LDH. Furthermore, isotherm, kinetics, and thermodynamic analyses were performed for the adsorption of BSA onto MCM-41@LDH under the optimized conditions designed by CCD experiments. It is revealed that the Freundlich model showed an excellent fit to the

Table 6. Thermodynamic Parameters of the BSA Adsorption onto MCM-41@LDH

Equation	T	ΔH°	ΔS°	ΔG°
$y = 373\,x - 0.2619$	288.15	-3101.12	-0.002	-3100.49
$R^2 = 0.9442$	298.15			-3100.47
	308.15			-3100.45
	318.15			-3100.43

T: temperature (K); ΔH°: enthalpy (kJ mol^{-1}); ΔS°: entropy (kJ mol^{-1}); ΔG°: Gibbs free energy (kJ mol^{-1} K^{-1}).

Table 7. Comparing the Adsorption of BSA onto MCM-41@LDH with other Adsorbents

Adsorbent	Kinetics model	Isotherm model	Equilibration time	q_{eq} (mg g^{-1})	n	K_F	Ref.
Graphene nanoplatelets	Second-order	Freundlich	24 h	76.9	0.21	96.4	[35]
Stearyl Alcohol- grafted-epichlorohydrin-grafted-aminopropyl silane triol functionalized with sulfonic acid	Second-order	Sips	3 h	35.12 (at 303 K)	-	-	[56]
MCM-41@LDH	Second-order	Freundlich	55 min	147.05	0.84	2.71	Current study

q_{eq}: the amount of BSA adsorbed at equilibration time (mg g^{-1}), n and K_f: Freundlich coefficients.

experimental data, indicating that the BSA adsorption onto MCM-41@LDH is heterogeneous. The adsorption process was also found to be favorable, as indicated by the value of 1/n > 1. The adsorption kinetics revealed the second-order model for the adsorption process. The negative values of ΔG° and ΔH° point to possibility and exothermic BSA adsorption, respectively. The low value of ΔS° indicates that BSA is a soft protein and dehydration of hydrophobic parts of protein has occurred. Based on the obtained results and comparison with other adsorbents, it is suggested that MCM-41@LDH may be a good support for chromatography applications in the field of BSA separation and purification.

ACKNOWLEDGEMENTS

The authors gratefully acknowledge the support of Yasouj University for this study.

REFERENCES

[1] P. Ghosh, J. Patwari, S. Dasgupta, J. Phys. Chem. B 121 (2017) 1758.
[2] P. Yang, Q. Liu, J. Liu, H. Zhang, Z. Li, R. Li, L. Liu, J. Wang, Ind. Eng. Chem. Res. 56 (2017) 3588.
[3] P. Hertzog, A. Shaw, J.L. Smith, R. Garner, J. Immunol. Methods 62 (1983) 49.
[4] M.M. Leong, G.R. Fox, Anal. Biochem. 172 (1988) 145.
[5] S. Birnbaum, S. Nilsson, Anal. Chem. 64 (1992) 2872.
[6] R. Sinibaldi, M.G. Ortore, F. Spinozzi, S. de Souza Funari, J. Teixeira, P. Mariani, Eur. Biophys. J. Biophy. 37 (2008) 673.
[7] R.A. Latour, Encyclopedia of biomaterials and biomedical engineering. 1 (2005) 270.
[8] D.G. Castner, B.D. Ratner, Surf. Sci. 500 (2002) 28.

[9] V. Hlady, J. Buijs, Curr. Opin. Biotech. 7 (1996) 72.
[10] W.B. Tsai, J.M. Grunkemeier, C.D. McFarland, T.A. Horbett, J. Biomed. Mater. Res. 60 (2002) 348.
[11] S.J. Geelhood, T.A. Horbett, W.K. Ward, M.D. Wood, M.J. Quinn, J. Biomed. Mater. Res. 81 (2007) 251.
[12] W. Kusnezow, J.D. Hoheisel, Biotechniques. 33 (2002) S14.
[13] Z. Wu, H. Chen, X. Liu, J.L. Brash, Macromol. Biosci. 12 (2012) 126.
[14] W. Norde, Colloid. Surface. B: Biointerfaces 1 (2008) 1.
[15] R.A. Latour, Colloid. Surface. B: Biointerfaces 191 (2020) 110992.
[16] J. Wang, X. Guo, J. Hazard. Mater. 390 (2020) 122156.
[17] A. Katiyar, L. Ji, P.G. Smirniotis, N.G. Pint, Micropor. Mesopor. Mat. 80 (2005) 311.
[18] S.A. Bhakta, E. Evans, T.E. Benavidez, C.D. Garcia, Anal. Chim. Acta 872 (2015) 7.
[19] G. Mishra, B. Dash, S. Pandey, Appl. Clay Sci. 153 (2018) 172.
[20] M. Mirzaei, M.B. Zarch, M. Darroudi, K. Sayyadi, S.T. Keshavarz, J. Sayyadi, A. Fallah, H. Maleki, Appl. Sci. 10 (2020) 7533.
[21] Z. Wu, D. Zhao, Chem. Comm. 47 (2011) 3332.
[22] A. Taguchi, F. Schüth, Micropor. Mesopor. Mat. 77 (2005) 1.
[23] V.V. Guliants, M.A. Carreon, Y.S. Lin, J. Membrane Sci. 235 (2004) 53.
[24] P.B. Sarawade, J.-K. Kim, H.-K. Kim, H.-T. Kim, Appl. Surf. Sci. 254 (2007) 574.
[25] A.B. Fuertes, Micropor. Mesopor. Mat. 67 (2004) 273.
[26] E. Tasciotti, X. Liu, R. Bhavane, K. Plant, A.D. Leonard, B.K. Price, M.M.-C. Cheng, P. Decuzzi, J.M. Tour, F. Robertson, M. Ferrari, Nat. Nanotechnol. 3 (2008) 151.
[27] M.V. Speybroeck, V. Barillaro, T.D. Thi, R. Mellaerts, J. Martens, J.V. Humbeeck, J. Vermant, P. Annaert, G.V. Den Mooter, P. Augustijns, J. Pharm. Sci. 98 (2009) 2648.
[28] B. Naik, N.N. Ghosh, Recent Pat. Nanotech. 3 (2009) 213.
[29] B.G. Trewyn, I.I. Slowing, S. Giri, H.-T. Chen, V.S.Y. Lin, Accounts Chem. Res. 40 (2007) 846.
[30] T. Heikkilä, J. Salonen, J. Tuura, M.S. Hamdy, G. Mul, N. Kumar, T. Salmi, D.Y. Murzin, L. Laitinen, A.M. Kaukonen, J. Hirvonen, V.P. Lehto, Int. J. Pharm. 331 (2007) 133.
[31] Y. Zhu, J. Shi, H. Chen, W. Shen, X. Dong, Micropor. Mesopor. Mat. 84 (2005) 218.
[32] N. Hao, F. Tang, L. Li, Micropor. Mesopor. Mat. 218 (2015) 223.
[33] Z.G. Peng, K. Hidajat, M.S. Uddin, Journal of Colloid and Interface Science. 271 (2004) 277.
[34] T. Kopac, K. Bozgeyik, Chem. Eng. Commun. 203 (2016) 1198.
[35] M. Seredych, L. Mikhalovska, S. Mikhalovsky, Y. Gogotsi, C J. Carbon Res. 4 (2018) 3.
[36] F. Karami, A. Shokrollahi, R. Razavizade, Adv. Mater. Lett. 12 (2021) 21101670.
[37] C. Kresge, M. Leonowicz, W.J. Roth, J. Vartuli, J. Beck, Nature 359 (1992) 710.
[38] M. Sharifi, A. Shokrollahi, F. Ebrahimi, Int. J. Environ. Anal. Chem. (2021) 1.
[39] M. Larizadeh, Master's Thesis. February 2020, Yasouj University, Yasouj, Iran.
[40] G. Hanrahan, K. Lu, Crit. Rev. Anal. Chem. 36 (2006) 141.
[41] G. Grigoropoulou, P. Stathi, M. Karakassides, M. Louloudi, Y. Deligiannakis, Colloid. Surface. A 320 (2008) 25.
[42] Q.-Z. Yang, Y.-Y. Chang, H.-Z. Zhao, Water Res. 47 (2013) 6712.
[43] L. Raki, J. Beaudoin, L. Mitchell, Cement and Concrete Res. 34 (2004) 1717.
[44] A.A. Tokmakov, A. Kurotani, K.-I. Sato, Front. Mol. Biosci. 8 (2021) 775736.
[45] K. Forough. PhD's Thesis. February 2023, Yasouj University, Yasouj, Iran.
[46] N.K. Amin, Desalination. 223 (2008) 152.
[47] A.K. Singh, Nanoparticle Ecotoxicology, in Engineered Nanoparticles, Academic Press, Boston, 2016.
[48] F. Haghseresht, G.Q. Lu, Energ. Fuel. 12 (1998) 1100.
[49] K. Fytianos, E. Voudrias, E. Kokkalis, Chemosphere. 40 (2000) 3.
[50] Y.S. Ho, G. McKay, Process Biochem. 34 (1999) 451.
[51] X.-S. Wang, Y. Qin, Process Biochem. 40 (2005) 677.
[52] Q. Hu, Z. Zhang, J. Mol. Liq. 277 (2019) 646.
[53] S. Lagergren, Kungliga svenska vetenskapsakademiens.

Handlingar. 24 (1898) 1.
[54] W. Gu, C.-j. Sun, Q. Liu, H.-x. Cui, Trans. Nonferrous Met. Soc. 19 (2009) s845.
[55] F.-C. Wu, R.-L. Tseng, R.-S. Juang, Chem. Eng. J. 150 (2009) 366.
[56] T.A. Rauf, T.S. Anirudhan, Mater. Today: Proc. 41 (2021) 728.